Journal of Cleaner Production 286 (2021) 124965

Contents lists available at ScienceDirect

Journal of Cleaner Production

journal homepage: www.elsevier.com/locate/jclepro

Spatiotemporal assessment of $PM_{2.5}$ concentrations and exposure in China from 2013 to 2017 using satellite-derived data

Qingqing He [a, b, 1, *], Ming Zhang [a, 1], Yimeng Song [c], Bo Huang [b, **]

[a] School of Resource and Environmental Engineering, Wuhan University of Technology, Wuhan, 430070, China
[b] Department of Geography and Resource Management, The Chinese University of Hong Kong, Hong Kong, China
[c] Department of Urban Planning and Design, The University of Hong Kong, Hong Kong, China

ARTICLE INFO

Article history:
Received 7 February 2020
Received in revised form
23 October 2020
Accepted 3 November 2020
Available online 12 November 2020

Handling editor: M.T. Moreira

Keywords:
$PM_{2.5}$ concentration
Health risk exposure
Spatiotemporal patterns
City scale
China

ABSTRACT

Satellite-based estimation of fine particulate matter of 2.5 μm or less ($PM_{2.5}$) at a high spatiotemporal resolution is important to understand the detailed dynamics of $PM_{2.5}$ pollution and exposure. Stricter clean air policies have been enacted in recent years to tackle China's serious problem with $PM_{2.5}$ pollution, including the implementation of the Air Pollution Prevention and Control Action Plan between 2013 and 2017. However, assessment of the change in national $PM_{2.5}$ exposure during this period is difficult due to the limitation of high-resolution $PM_{2.5}$ data. To address this issue, a satellite-based spatiotemporal model was developed to predict daily high-resolution surface $PM_{2.5}$ concentrations in China during the designated period, and quantitative analysis was then performed regarding the spatiotemporal characteristics of this critical pollutant. The corresponding changes in the population exposure to $PM_{2.5}$ were also explored at a fine scale. The overall concentrations of $PM_{2.5}$ declined from 2013 to 2017, with substantial decreases in eastern China but negligible decreases in western China. The national $PM_{2.5}$ concentration declined remarkably from 2013 to 2014 to 2015–2017. The Beijing–Tianjin–Hebei and Pearl River Delta regions and most cities reached the goals set by the Air Pollution Prevention and Control Action Plan. However, despite the overall reduction in the $PM_{2.5}$ concentration, by 2017 the vast majority of the Chinese population still lived in areas with sustained levels of high risk from fine particle pollution. The findings from this study have crucial environmental policy implications for the mitigation of $PM_{2.5}$ pollution and could benefit $PM_{2.5}$–related health studies in China.

© 2020 Elsevier Ltd. All rights reserved.

1. Introduction

Fine particulate matter ($PM_{2.5}$) consists of aerosolized particles with an aerodynamic diameter of 2.5 μm or less. $PM_{2.5}$ is an air pollutant that has adverse effects on public health and on the environment and leads to increased morbidity in the form of cardiovascular disease (Barnett et al., 2006), respiratory problems (Schwartz 1996), and even premature death (Chen et al., 2013; Gu et al., 2018). It has been reported that each increase of 100 μg/m^3 in the respirable suspended particle concentration is associated with a 14% increase in the all-cause mortality rate (Chen et al., 2013). Another study reported that $PM_{2.5}$ pollution is associated with 87,000 deaths each year in China (Gu et al., 2018). $PM_{2.5}$ has thus become a focal issue that has attracted concern from the public, scientific researchers, and policymakers.

In recent years, China's rapid economic growth has been associated with serious air pollution, of which $PM_{2.5}$ is the dominant pollutant (Fang et al., 2014; Li et al., 2017; Wang et al., 2020; You et al., 2017). This pollution has raised unprecedented concern, which has led China to take a series of steps in recent years to fight air pollution (Lin et al., 2018). When the new national ambient air quality standards (NAAQS) were issued in 2012, the $PM_{2.5}$ mass concentration was included as an essential air quality indicator, with mean daily and annual limits of 75 and 35 μg/m^3, respectively. A number of ground-based air quality monitoring stations have been deployed nationwide since 2013 and together comprise the national ambient air quality observation network. The Air Pollution Prevention and Control Action Plan (APPCAP) was implemented between 2013 and 2017, with a focus on reducing $PM_{2.5}$ pollution

* Corresponding author. School of Resource and Environmental Engineering, Wuhan University of Technology, Wuhan, 430070, China.
** Corresponding author. Department of Geography and Resource Management, The Chinese University of Hong Kong, Shatin, Hong Kong.
E-mail addresses: qqhe@whut.edu.cn (Q. He), bohuang@cuhk.edu.hk (B. Huang).
[1] Qingqing He and Ming Zhang are co-first authors.

https://doi.org/10.1016/j.jclepro.2020.124965
0959-6526/© 2020 Elsevier Ltd. All rights reserved.

(The State Council of China, 2013). It is vital to assess the changes in $PM_{2.5}$ concentration and exposure that occurred over this 5-year period to establish the effectiveness of the current air pollution control policies, to guide future action, and to inform epidemiological studies. In addition, because $PM_{2.5}$ pollution is a shared environmental issue due to long-range transboundary air pollution, it is important to compare the current situation of ambient $PM_{2.5}$ pollution in China with other countries, such as the United States.

Several studies have investigated the changes in $PM_{2.5}$ exposure across China from 2013 to 2017 with the use of chemical transport models (Cai et al., 2017; Zhang et al., 2019), ground observations (Huang et al., 2018), and satellite-derived estimates (Gui et al., 2019; Xue et al. 2019a, 2020). These studies found an overall reduction in the $PM_{2.5}$ level from 2013 to 2017 but also found significant spatiotemporal variations. However, most studies that focused on 5-year $PM_{2.5}$ exposure relied on coarse-resolution $PM_{2.5}$ data or fixed monitoring station data. Because the particles suspended in the air frequently vary over a very small spatial scale, the air quality and epidemiological communities have advocated for the collection of $PM_{2.5}$ data at a higher spatial resolution to provide additional information that may be missed by coarse-resolution data, such as smoke plumes and detailed gradients within urban areas (Remer et al., 2013). Therefore, it is of great importance to explore the spatiotemporal heterogeneity in $PM_{2.5}$ exposure with the use of high-resolution $PM_{2.5}$ data and to reveal local contrasts that would be missed by coarse-resolution $PM_{2.5}$. Such exploration would improve our characterization of local pollution changes and thus benefit health-related studies and policymaking.

Since the release of the Moderate Resolution Imaging Spectroradiometer (MODIS) global 3-km resolution aerosol product (Levy et al., 2013), an increasing number of studies in China have used the fine-resolution aerosol optical depth (AOD) product to reconstruct surface $PM_{2.5}$ levels and explore the spatiotemporal characteristics of specific regions (Guo et al., 2017b; He et al., 2018a; Lin et al., 2018; Yang et al., 2019). He and Huang (2018b) used this product and the national air-quality monitoring network to devise a geographically and temporally weighted regression (GTWR) model to predict the daily nationwide $PM_{2.5}$ at a fine spatial scale for China for 2015. The validation results showed highly accurate ground $PM_{2.5}$ estimates ($R^2 = 0.80$). Xiao et al. (2017) and Liang et al. (2018) applied the 1-km aerosol product by Multi-angle Implementation of Atmospheric Correction (MAIAC) to estimate the daily $PM_{2.5}$ levels in the Yangtze River Delta (YRD) and in Beijing, China. However, although a handful of studies have predicted fine-scale $PM_{2.5}$ concentrations for specific regions (Lin et al., 2018; Ma et al., 2016; Wu et al., 2016; Xiao et al., 2017; Liang et al., 2018) or for only 1 year (Wei et al., 2019, 2020), few data on the national $PM_{2.5}$ concentrations at a high spatial resolution are available for 2013 to 2017, which has led to limited long-term research on $PM_{2.5}$ changes throughout China. In addition, the lack of such data makes it difficult to uncover the differences between fine vs. coarse resolution in the assessment of $PM_{2.5}$ exposure.

Previous studies assessed exposure on the basis of the population-weighted mean $PM_{2.5}$ concentration to investigate the average level of exposure to $PM_{2.5}$ for a specific region (He and Huang 2018a; van Donkelaar et al., 2016; Xie et al., 2015). Peng et al. (2016) analyzed the health threat from $PM_{2.5}$ exposure for China from 1999 to 2011 by multiplying the $PM_{2.5}$ levels by the population size. An examination of the population-weighted mean $PM_{2.5}$ concentration is preferable to an analysis of the spatially averaged concentration because the domain-averaged value unweighted by population would likely underestimate the average exposure and hence underrate the health effects of $PM_{2.5}$ exposure accordingly (van Donkelaar et al., 2016; Xie et al., 2015). Due to data availability, most exposure assessment studies have used consistent population distribution data (e.g., the Chinese national 1-km grid population density dataset) for the entire study period (He and Huang 2018a; Peng et al., 2016; Xie et al., 2015). However, because people are mobile across space and over time, it would also be meaningful to examine the sensitivity of the exposure assessments to demographic changes.

An in-depth investigation of the dynamic characteristics of $PM_{2.5}$ exposure during the introduction of stricter clean air policies in China, whose people suffer from some of the world's most severe $PM_{2.5}$ pollution, would facilitate environmental policymaking and the assessment of the impact of $PM_{2.5}$ on health. Therefore, this study was intended to predict daily high-resolution $PM_{2.5}$ concentrations from 2013 to 2017 with the use of a spatiotemporal regression model. Then, aided by this high-resolution dataset, the spatiotemporal dynamics of fine-particle pollution for mainland China were investigated. The overall spatial and temporal changes in the potential health risk due to ambient $PM_{2.5}$ pollution were also explored from an alternate view, that is, exposure assessment by linking population to the $PM_{2.5}$ concentration. This report concludes with a discussion of the effects of the spatiotemporal scale on the assessment of $PM_{2.5}$ exposure.

2. Data and methods

2.1. Satellite-based $PM_{2.5}$ inference

In this study, we re-developed a GTWR model used in our previous work (He and Huang 2018b) to produce daily $PM_{2.5}$ estimates at the fine 3-km grid scale from 2013 to 2017. Details of the GTWR modeling used to infer high spatial resolution $PM_{2.5}$ predictions for each day over all of China from satellite remote sensing have been reported in He and Huang (2018b) and briefly summarized here. GTWR is an extension of the popular geographically weighted regression model for elucidating nonstationary spatiotemporal data via a three-dimensional weighting mechanism. The standard structure of the GTWR model regarding response variable Y and explanatory variable X_m is described as Eq. (1) (Huang et al., 2010):

$$Y_k = \alpha_0(\mu_k, \nu_k, \tau_k) + \sum_m \alpha_m(\mu_k, \nu_k, \tau_k) X_{km} + \varepsilon_k \tag{1}$$

where (μ_k, ν_k, τ_k) is the spatiotemporal coordinate for sample *k:* (μ_k, ν_k) refers to geolocation and τ_k refers to time. The spatiotemporal intercepts α_0 and slopes α_m are linked to the weight matrix (**W**) that is used to explain the effect of the estimated points to other samples regarding space and time. The diagonal elements ω_{kl} of the spatiotemporal weight matrix **W** can be defined as in Eq. (2) (He and Huang 2018b). The spatiotemporal bandwidth η_{ST} and scale factor ϕ are core parameters that determine the spatiotemporal weighting value, which can be obtained by computing the sum of squared errors, as in Eq. (3) (Huang et al., 2010).

$$\omega_{kl} = \exp\left(-\frac{\left[(\mu_k - \mu_l)^2 + (\nu_k - \nu_l)^2\right] + \phi(\tau_k - \tau_l)^2}{(\eta_{ST})^2} \right) \tag{2}$$

$$\mathrm{CVRSS}(\eta_{ST}; \phi) = \sum_k \left(y_k - \hat{y}_{\neq k}(\eta_{ST}; \phi) \right)^2 \tag{3}$$

In this study, Y_k refers to the ground-level $PM_{2.5}$ value of the space-time sample *k* at geographic coordinate (μ_k, ν_k) and temporal location τ_k, and α_0 represents the location-time-specific intercept for sample *k*. The fused AOD (see Table S1 for the detail about how to obtain the fused AOD) was used as the primary variable because the models with satellite AOD performed better than those without this input (Table S2), in line with previous findings (Hu et al., 2014; Lee et al., 2016). Seven ancillary explanatory variables including RH, TMP, WDS, PBLH, NDVI, DEM, and PAS (details of the ancillary variables are given in Table S1) were also used for spatiotemporal modeling. To predict the daily mean values of $PM_{2.5}$ concentrations for a 3 × 3 km grid, the explanatory variable data with various spatial resolutions and temporal intervals were reprocessed using interpolation and aggregation methods. Table S2 also indicates no significant collinearity problem in the current model because the condition index was less than 30 when the 8 variables were input into the model. The (μ_k, ν_k) and τ_k denote the center coordinate of a grid cell and the day of the year for sample k, respectively, and ε_k is the error term for sample k.

In the GTWR calibrating, two GTWR models were separately established for eastern and western China with the same model structure to derive daily ground $PM_{2.5}$ for the entire mainland China due to the large area of the study region and the uneven distribution of $PM_{2.5}$ monitoring stations (He and Huang 2018b). Eastern and western China were partitioned according to Aihui-Tengchong Line, the dividing line in the Chinese population proposed by Hu Huangyong in 1935. A fixed bandwidth regime was used to retrieve the spatiotemporal bandwidth η_{ST} for each GTWR. A 10-fold cross-validation (CV) technique was executed to examine the potential model overfitting problem. In the GTWR prediction process, we adjusted the model parameters to generate reliable $PM_{2.5}$ predictions for areas far from the monitors (e.g., the northernmost part of Xinjiang and the northeastern corner of Heilongjiang) because the model that was dependent upon the available sample dataset did not produce robust estimations for these remote regions. Finally, surface $PM_{2.5}$ values over the whole of China from 2013 to 2017 were predicted on a daily basis, which excluded Hong Kong, Macau and Taiwan, due to data availability. Fig. S3 shows the descriptive statistics and histograms for the measured $PM_{2.5}$, fused AOD, and other explanatory variables used in the GTWR modeling.

2.2. Analytical methods

Taking advantage of the daily high-resolution $PM_{2.5}$ predictions, mean monthly and annual $PM_{2.5}$ concentrations were calculated for each pixel in MATLAB 2016b, and corresponding spatial distributions were mapped in ArcGIS 10.4 for subsequent spatiotemporal analysis. Pixel-based linear trend analysis was applied for the 5-year study period using least-squares regression, in which the fitted slope represents the trend in $PM_{2.5}$ change. Trends (ω) were regarded as statistically significant at a confidence level of 95% when $|\omega/\sigma| > 2$ (Tiao et al., 1990), where σ is the standard deviation computed in accordance with Weatherhead et al. (1998). Regional analysis was also performed by extracting the domain-average $PM_{2.5}$ values for each month and year in the 5-year timespan.

Standard deviation ellipse (SDE) analysis was performed using “Spatial Statistics Tools” in ArcGIS 10.4. SDE is a statistical approach that expresses the overall spatial characteristics of a set of discrete points (Wang et al., 2015). Aided by parameters such as the average center and standard distance calculated in SDE, an abstract view of the moving track of national $PM_{2.5}$ changes was created by drawing the annual ellipses and average centers of satellite-derived $PM_{2.5}$ over China across a time series on a map, which helped to summarize the spatial dynamic process of national $PM_{2.5}$ variation.

3. Results

3.1. Evaluation of satellite-based $PM_{2.5}$ estimates

Fig. 1 shows the GTWR scatterplots and 10-fold cross-validation results against ground-level $PM_{2.5}$ observations collocated at each spatiotemporal coordinate for which estimated $PM_{2.5}$ values were available. The $PM_{2.5}$ concentrations predicted by the spatiotemporal model for 2013 to 2017 showed good agreement with the ground measurements in both the model development and CV processes, accounting for 86% and 81%, respectively, of the variability in the surface $PM_{2.5}$ estimation for each day over the entire study area. A slight overfitting problem was identified by comparing the results of the model development and validation (e.g., the difference in R^2 between the two processes was 0.05). The daily spatial autocorrelation was examined by computing the global Moran’s I index using ArcGIS 10.4, which found no significant spatial autocorrelation in the residuals of each estimation day. In addition, the 3-km $PM_{2.5}$ predictions reconstructed by GTWR achieved a modeling accuracy comparable with studies that have used 1-km MAIAC AOD data (CV $R^2 = 0.62{-}0.84$) (Chudnovsky et al., 2014; Hu et al., 2014; Liang et al., 2018; Xiao et al., 2017). These results suggest that the $PM_{2.5}$ estimates reconstructed in this study were generally reliable and show promise for revealing the spatiotemporal changes in population exposure to $PM_{2.5}$ in China over the 2013−2017 period.

Fig. S4 provides further details about the space-time characteristics of the performance during spatiotemporal modeling. More than 73% of the monitoring sites fell within the bias level of ±5 μg/m^3, indicating a good agreement between observed and predicted $PM_{2.5}$ on days when fused AODs were available during the study period (Fig. S4 (a)). According to Fig. S4 (b), the multiyear average local R^2 value for each grid cell ranged from 0.72 to 0.99, with 98% of values above 0.80. The spatially averaged residual values for each day ranged from −27 to 29 μg/m^3, with more than 88% below ±5 μg/m^3; and the grid−cell mean values of local R^2 varied from 0.54 to 0.99, with more than 99% of daily local R^2 values above 0.80 (Fig. S4 (c)). These spatial and temporal changes in the mean residual and RMSE for each grid cell or day show that the performance of the GTWR model built in this study was quite stable across the whole of China, and accounted for a great amount of the spatiotemporal variability in the relationship between $PM_{2.5}$ and AOD.

3.2. Spatiotemporal variations in $PM_{2.5}$ concentrations

3.2.1. Temporal trends of $PM_{2.5}$ distribution

Fig. 2 shows the temporal evolution of spatially resolved $PM_{2.5}$ concentrations that were mapped from satellite remote sensing data at a 3-km resolution across China from 2013 to 2017. The annual average national $PM_{2.5}$ concentration declined from 45 to 36 μg/m^3 over the period, by a mean rate of −5% per year (Fig. 2 (a)−(e)). This reduction is consistent with the change in aerosol loading in China (He et al., 2019) and with previous $PM_{2.5}$-related studies (Bai et al., 2019; Cai et al., 2017; Lin et al., 2018; Xue et al., 2019). Areas of China that met this secondary level of national air quality standard (35 μg/m^3 of annual mean value) gradually expanded from parts of western China, Heilongjiang, and Yunnan provinces and eventually reached the low-$PM_{2.5}$ areas in parts of Sichuan, Chongqing, Shaanxi, Hubei, Liaoning, and Jilin provinces. In 2013, more than 64% of areas in China had $PM_{2.5}$ concentrations that exceeded the 35 μg/m^3 standard, but this figure decreased to ~45% by 2017. The overall reduction in $PM_{2.5}$ pollution in recent years suggests a general improvement in the atmospheric environment.

Fig. 2 (g) presents the spatial pattern of monthly variation in the

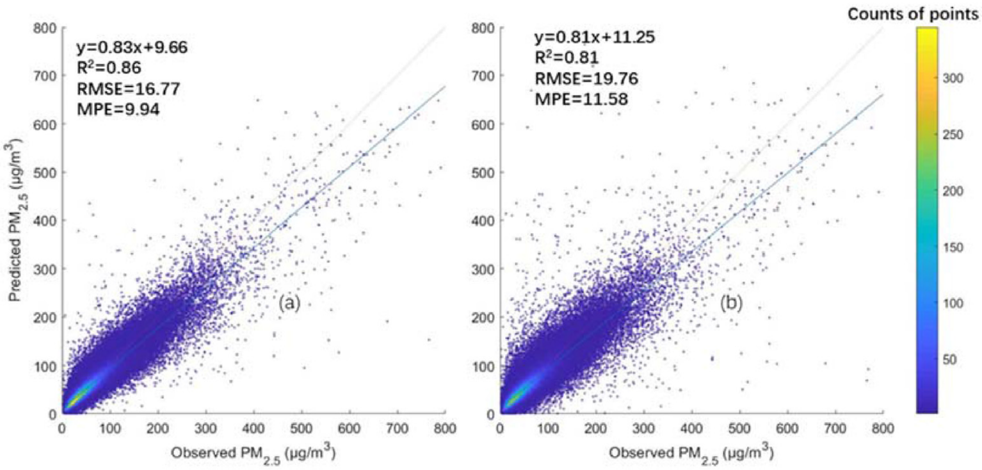

Fig. 1. Scatterplots for GTWR model development (a) and 10-fold CV (b) results between observed and inferred $PM_{2.5}$ values. The solid blue line shows the linear trend between observed and estimated $PM_{2.5}$ concentrations; the dotted orange line represents 1:1 line as a reference. RMSE and MPE stand for root mean square error and mean prediction error, respectively. (For interpretation of the references to colour in this figure legend, the reader is referred to the Web version of this article.)

$PM_{2.5}$ level at a 3-km resolution from 2013 to 2017, indicating substantial spatial variability in the $PM_{2.5}$ trend across China, although the overall $PM_{2.5}$ change was negative over the five years. Specifically, there was a decreasing tendency mainly to the east of the Aihui-Tengchong Line. A notable decline occurred in the densely populated areas, such as the Beijing-Tianjin-Hebei (BTH), Sichuan Basin (SCB), and central China regions. In 2013, the heavily polluted areas with annual mean values greater than 55 μg/m^3 included most of Hebei, Tianjin, Shandong, Henan, Anhui, Jiangsu, Shanghai, Hubei, Hunan, Guangxi, and Guangdong and parts of Shanxi, Shaanxi, Sichuan, Guizhou, and Jiangxi. By 2017, a sharp reduction of between 10 and 40 μg/m^3 in the $PM_{2.5}$ concentration had reduced these heavily polluted areas to most of Shandong and parts of Hebei, Henan, Anhui, Shanxi, Jiangsu, and Hubei.

In contrast, a small variation in the $PM_{2.5}$ concentration occurred in areas west of this line during the study years. From 2013 to 2016, there was virtually no change in the $PM_{2.5}$ concentration across almost all of western China, and the values over part of the Tarim Basin and western Inner Mongolia, Gansu, and Sichuan changed little in 2017. However, despite a significant descending trend over eastern China throughout the 5-year study period, concentrations in the east in 2017 tended to be higher than those in the west (e.g., an annual mean $PM_{2.5}$ concentration of 39 μg/m^3 for the eastern areas vs. 34 μg/m^3 for the western areas), which suggests that high $PM_{2.5}$ concentrations in the densely populated and highly urbanized regions remained higher than those in less-populated western areas.

The results of the SDE analysis using high-resolution $PM_{2.5}$ estimates (Fig. 3) summarize the overall temporal changes in the spatial distribution of $PM_{2.5}$ across China over the study period. The standard deviation ellipse, which includes the most elements, shows that fine-particle pollution in China was concentrated mainly in the central and eastern areas. This suggests that the central and eastern areas made the predominant contribution to the collective amount of fine particulate matter throughout China over the 5 years. The long axis of the standard deviation ellipse increased from 1677 km in 2013 to 1706 km in 2017, whereas the short axis declined slightly from 1085 km to 1080 km. The minimal lengthening of the major axis with almost no change in the minor axis of the ellipse indicates a weak expansion tendency in the spatial variation of $PM_{2.5}$ concentrations over time. The median center of the annual national $PM_{2.5}$ levels was located in Gansu province and moved less than 100 km throughout the time span, indicating an insignificant change in the median center. An obvious change in $PM_{2.5}$ in a specific region over time would trigger the general movement of the average center in a specific direction. The lack of a clear direction in the center shift in Fig. 3 thus implies that $PM_{2.5}$ concentrations in different regions changed inconsistently over time.

Also, it is clear from tracking the changes in the two axes and the movement of the annual center over the 5-year period that the spatial variations in $PM_{2.5}$ were uneven over time, although the overall directional trend of the standard deviation ellipse was obviously northwestward. The annual values of these indicators (e.g., the length of the major and minor axes and the median center) did not increase or decrease consistently. For example, the average center of $PM_{2.5}$ in 2017 was southeast of that in 2016 (longitude 103.45°, latitude 36.37°), whereas the center in 2014 (104.68°, 36.20°) was northeast of that in 2013. The uneven pattern is attributable mainly to substantial differences in $PM_{2.5}$ changes over space and time, which can be identified in Fig. 2.

3.2.2. APPCAP and $PM_{2.5}$ reduction

This study focused on fine-particle pollution during the 2013–2017 period in which the APPCAP was implemented. The APPCAP aimed to reduce particle pollution according to baseline pollution levels in different regions in 2013: (1) $PM_{2.5}$ concentrations in prefecture-level cities should decrease by 10% from 2012 to 2017, with a corresponding decrease in the number of heavily polluted days; (2) over the same period, $PM_{2.5}$ levels in the BTH, YRD, and Pearl River Delta (PRD) regions should be reduced by 25%, 20%, and 15%, respectively (The State Council of China 2013).

To evaluate its effects, the overall $PM_{2.5}$ changes in terms of regional and city scale were summarized. Overall, the $PM_{2.5}$ estimates in the BTH, YRD, and PRD regions declined by 27.87%, 19.40%, and 20.44%, respectively (Table 1). Meanwhile, more than 80% of cities showed a 10% decrease in the annual mean $PM_{2.5}$ concentration, whereas the number of days with concentrations above 75 μg/m^3 decreased from 42 in 2013 to 25 in 2017 (Fig. S5). These findings suggest that APPCAP offered an effective approach to alleviating fine-particle pollution in most of China because the BTH and PRD regions and most cities reached the goals set by the APPCAP. However, these findings also show that the $PM_{2.5}$ pollution levels in these major regions during 2017 were far from the Level 2

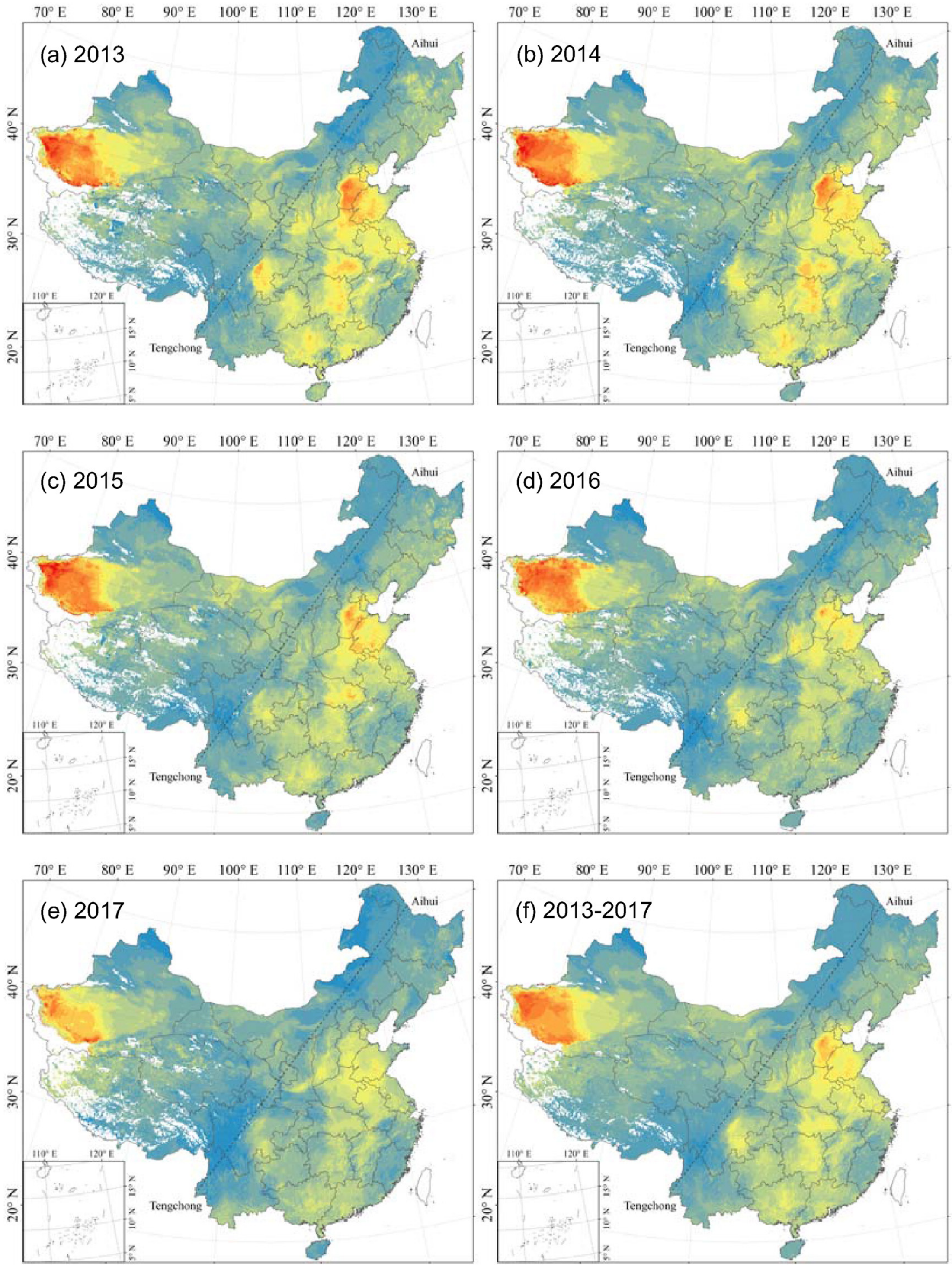

Fig. 2. Spatial distribution of mean $PM_{2.5}$ concentrations over China for the five study years (2013–2017) (a)–(f) and (g) the spatial distribution of the statistically significant trend of mean monthly $PM_{2.5}$ concentrations in China from 2013 to 2017. Linear trends for (g) all had p values below 0.05, and the insignificant slopes are labeled in white. Hong Kong, Macau and Taiwan were excluded in the spatiotemporal prediction due to data availability.

limit of the national air quality standards.

3.3. *Spatiotemporal assessment of health risk from $PM_{2.5}$ exposure*

3.3.1. *Overall changes in $PM_{2.5}$ exposure*

Because the health effects of population exposure due to ambient $PM_{2.5}$ have been defined as the product function associated with the particulate level and population size (Peng et al., 2016), this study quantitatively assessed the health risk from an alternative perspective of the population-weighted mean $PM_{2.5}$ concentration, which integrates the estimated concentration with the national population distribution (Fu et al., 2014; see Fig. S6 for population distribution). Fig. 4 shows the temporal variations in the proportion of the Chinese population exposed to various $PM_{2.5}$ levels over the 5-year time span. It is clear that more than 80% of the Chinese population was exposed to a harmful environment in which $PM_{2.5}$ levels exceeded the 35 μg/m^3 standard, and more than 99% of the population lived in environments in which $PM_{2.5}$ values exceeded the NAAQS Level 1 and World Health Organization (WHO) Interim Target (IT)-1 limit of 15 μg/m^3. These results show that almost none of the Chinese population escaped long-term exposure to risky levels of fine-particle pollution, which is a serious health threat for China.

As shown in Fig. 4 (a), the percentage of the total population exposed to dangerous fine-particle pollution declined in each consecutive year from 2013 to 2017. The proportion of the population exposed to serious levels above 75 μg/m^3 declined sharply from 25.43% in 2013 to 1.19% in 2017, whereas the proportion exposed to high concentrations above 55 μg/m^3 decreased from 65.70% to 34.13% over the same period. The greatest decline in the cumulative percentage of the population exposed to $PM_{2.5}$ was observed at a concentration of 62 μg/m^3, which decreased from ~37% to 16.73% over the 5-year period, a decline of nearly 70%. A small proportion (17.54%) of the national population in 2017 lived in areas in which the $PM_{2.5}$ levels satisfied the secondary air quality standard of 35 μg/m^3, although this represents an increase of ~11% from 6.77% in 2013. These findings suggest that despite the dramatic reduction from the higher $PM_{2.5}$ levels (e.g., >55 μg/m^3), the vast majority of the Chinese population was consistently exposed to risky fine-particle levels above the 35 μg/m^3 standard during the 2013–2017 period.

Fig. 4 (b)–(c) illustrates the year-to-year distribution of $PM_{2.5}$ estimates according to population and population density over China from 2013 to 2017. In general, the national $PM_{2.5}$ concentrations fell between 35 and 85 μg/m^3 (Fig. 4 (b)), and the high $PM_{2.5}$ concentrations usually occurred in densely populated regions, with two peaks for population densities of ~500 and ~10,000 people per km^2 (Fig. 4 (c)). The national $PM_{2.5}$ values changed remarkably from 2013 to 2014 to 2015–2017. National concentrations of 55–85 μg/m^3 were dominant in 2013–2014 and typically declined to 35–70 μg/m^3 over the following 3 years (Fig. 4 (b)). Heavily populated areas also experienced a discernible decrease from 65 to 70 μg/m^3 in the first 2 years to 50–60 μg/m^3 in 2015–2017 (Fig. 4 (c)). These findings imply that the discernible improvement in China's air quality probably began in 2015.

3.3.2. City-level spatial variations in annual $PM_{2.5}$ exposure

Satellite-derived high-resolution $PM_{2.5}$ data can be used to identify substantial spatial variability by calculating the population-weighted mean $PM_{2.5}$ concentration at a finer city-level spatial scale (Fig. 5). In general, the annual national population-weighted mean $PM_{2.5}$ concentrations were 63, 62, 55, 51, and 48 μg/m^3 for each year from 2013 to 2017, ~4–6 times higher than the WHO air quality guideline (AQG) of 10 μg/m^3 and ~1.4–1.8 times higher than the 35-μg/m^3 recommended by WHO IT-1 and NAAQS Level 2. Over the study period, 71 cities, primarily in Tibet, Yunnan, and northern Xinjiang, met the 35-μg/m^3 $PM_{2.5}$ standard, and one city, Diqing in Yunnan, had an annual $PM_{2.5}$ concentration below 15 μg/m^3 (Fig. 5(a)). However, 146 cities concentrated in eastern China and southern Xinjiang suffered severe $PM_{2.5}$ pollution above 55 μg/m^3 (Fig. 5 (a)).

Fig. 5 (b) and (c) present the temporal changes in the spatial distribution of the yearly population-weighted average $PM_{2.5}$ concentrations between 2013 and 2017. The figures show a notable reduction in large-concentration areas, indicating that the high $PM_{2.5}$ exposure declined significantly. In 2013, 186 cities had high $PM_{2.5}$ exposure (>55 μg/m^3), including those in southern Xinjiang and most of eastern China (excluding cities located in Heilongjiang, Jilin, Liaoning, and Fujian provinces). By 2017, little change was seen in the high $PM_{2.5}$ exposure in southern Xinjiang, but a massive decrease was seen in both the size and magnitude of the population-weighted averages in eastern China. The number of high-exposure cities (>55 μg/m^3) in eastern China shrank from 177 in 2013 to 89 in 2017, and only 19 cities in this area had a level above 65 μg/m^3. As the national particle concentration decreased from 2013 to 2017, the concentrations weighted by population in most of China were correspondingly reduced, resulting in mitigation of the health threat to varying degrees, especially in most cities in eastern China.

According to the population-weighted mean $PM_{2.5}$ concentrations in Fig. 5 (b) and (c), the number of cities that met the secondary air quality standard increased significantly from 39 in 2013 to 112 in 2017. However, these cities were mainly in sparsely populated areas in western and northeastern China, such as Yunnan, Qinghai, and Jilin provinces. Almost none of the major metropolitan areas, such as those in the BTH, YRD, and PRD regions, satisfied the 35 μg/m^3 standard, as confirmed in Table 2. Until 2017, more than 94% of the population in the BTH, YRD, PRD, and central China regions were exposed to fine-particle pollution above 35 μg/

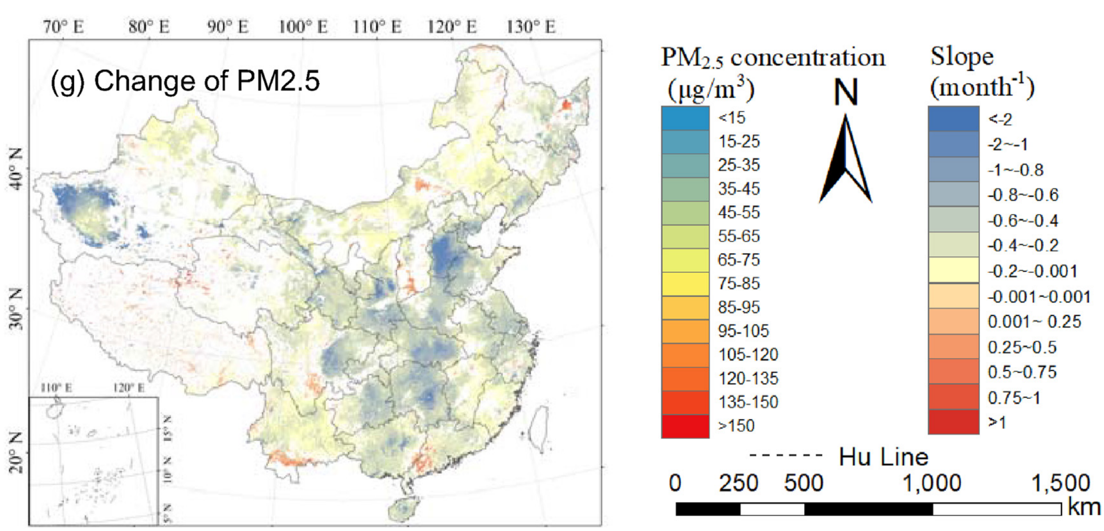

Fig. 2. (*continued*).

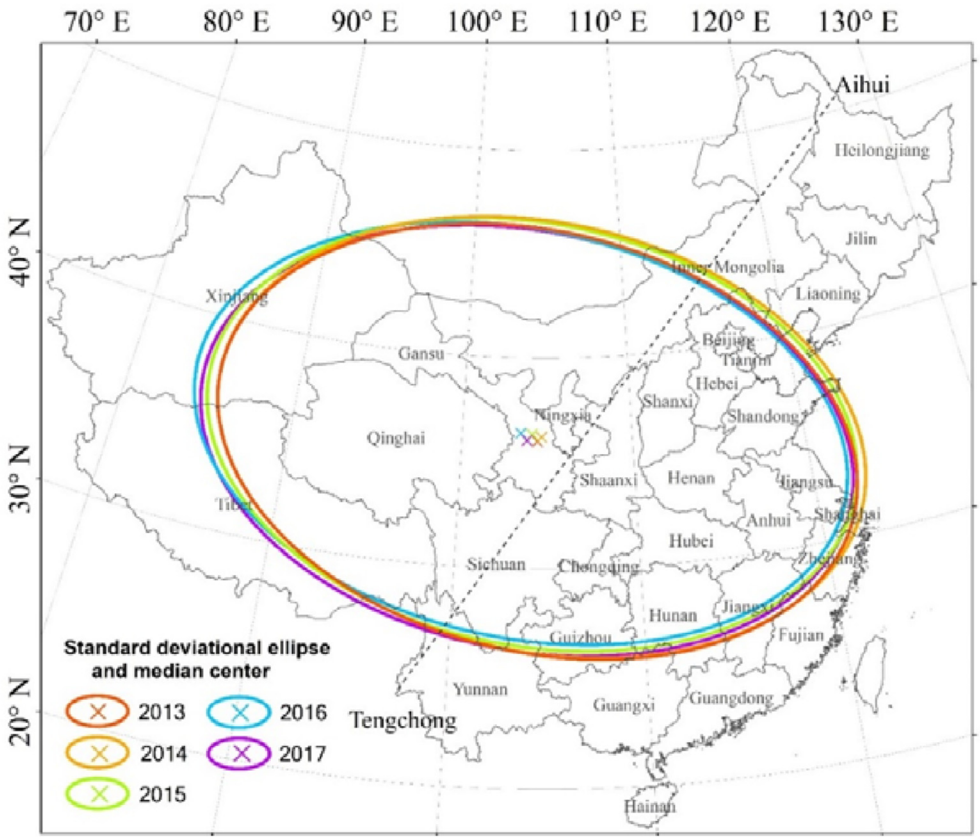

Fig. 3. Spatial changes in standard deviation ellipse and median center of satellite-derived $PM_{2.5}$ concentrations in China over the 5-year time span of 2013–2017.

Table 1
Annual mean $PM_{2.5}$ concentrations and severely polluted days in 2013 and 2017.

Region	Estimated PM2.5			Polluted days (PM2.5 > 35/75 μg/m^3)		
	2017	2013	Decreased by (%)	2017	2013	Decreased by
BTH	47.28	65.55	27.87	242/53	271/129	29/76
YRD	46.93	58.22	19.40	211/37	246/86	35/49
PRD	49.47	62.19	20.44	142/5	158/29	16/24

m^3. Thus, there is still a high health risk arising from fine-particle pollution in most Chinese cities, especially in densely populated areas, despite the overall mitigation of the most severe health risks from $PM_{2.5}$.

4. Discussion

4.1. Effect of spatial scale on $PM_{2.5}$ exposure assessment

To investigate the effects of the spatial scale of the $PM_{2.5}$ data sampling on the exposure assessment, the fine-scale $PM_{2.5}$ predictions and population distribution data were reconfigured into grids with coarser spatial resolutions of 15 × 15 km and 30 × 30 km. Fig. 6 shows that the 5-year population-weighted average $PM_{2.5}$ value over the entire study area derived from the high-resolution data was 56.1 μg/m^3, and the corresponding values were 55.4 and 54.6 μg/m^3 for the 15- and 30-km data, respectively. In most provinces, the mean concentrations from the coarse-resolution $PM_{2.5}$ data were lower than those from the high-resolution data. These findings suggest that the use of coarse-resolution $PM_{2.5}$ data is likely to result in systematic underestimation of $PM_{2.5}$ exposure.

To further demonstrate the benefits of fine-scale $PM_{2.5}$ data, the city- and province-level distributions of the population-weighted mean $PM_{2.5}$ concentrations were compared (Fig. S7). The map of provincial $PM_{2.5}$ exposure clearly generalizes the city-level distribution, losing considerable spatial detail and overestimating the less-exposed cities while underestimating the heavily exposed areas in most provinces. Population exposure shows great spatial variability within a province, but the population-weighted value averaged over large areas at the provincial level cannot represent the substantial spatial variations. It thus highlights the importance of fine-scale $PM_{2.5}$ for accurate assessment of pollution exposure.

4.2. Effects of population distribution on $PM_{2.5}$ exposure assessment

To evaluate the effects of the demographic data on $PM_{2.5}$ exposure, we compared the spatial average of the satellite-derived $PM_{2.5}$ concentrations, without considering the spatial distribution of the population data, with the city-level distribution of the population-weighted average $PM_{2.5}$ (Fig. 7). More than 300 cities had larger population-weighted mean values than these simple spatial averages, and positive discrepancies (>5 μg/m^3) were evident in 56 cities, primarily in eastern China and southern Xinjiang, including Beijing, Baoding, and Shijiazhuang (Hebei province), Wuhan (Hubei province), and Kashgar (Xinjiang). These results indicate that the population distribution strategies, especially in eastern China and southern Xinjiang were not conducive to improving air pollution.

In this study, as in most previous studies (Guo et al., 2017a; Xie et al., 2015), temporally constant population data were used to examine the annual changes in the population exposure to $PM_{2.5}$

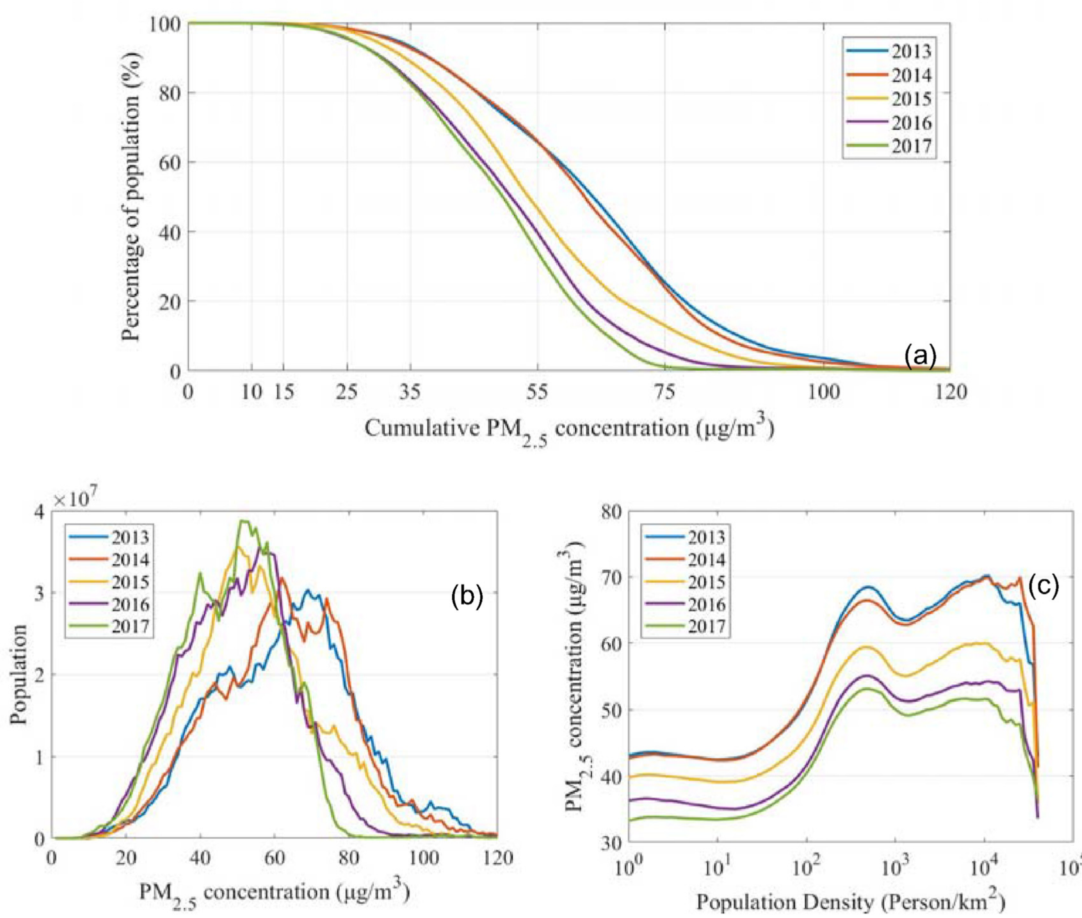

Fig. 4. Changes in $PM_{2.5}$ concentrations derived from satellite remote sensing from 2013 to 2017 according to (a) cumulative percentage of exposed population, (b) population, and (c) population density throughout China.

because it is difficult to obtain highly accurate population distribution data with a fine temporal interval. However, people are mobile across space and time, and the use of static population data cannot characterize the temporal dynamics of population distribution, which could distort the environmental effects on public health. Thus, temporal variation in the population distribution was introduced to explore whether population mobility has a significant effect on the assessment of $PM_{2.5}$ exposure. Monthly mean population data for eastern and southern China for February to May 2016 were retrieved from mobile phone location-request data and used to identify variations in the population-weighted mean $PM_{2.5}$ over these 4 months. The data source and processing method for the mobile population data were summarized in our previous study (Chen et al., 2018). Fig. 8 compares city-level population-weighted average $PM_{2.5}$ values computed from static and dynamic population data. Over the 4 months, there was very little change in the static-vs. dynamic-based values in around 58%–68% of the 240 cities, with a difference of less than ±5%, and more than 80% of cities had a difference between −10% and 10%. These results indicate that on a monthly timescale, the population distribution has little influence on exposure to $PM_{2.5}$, which implies that the long-term effects of demographic dynamics on assessed $PM_{2.5}$ exposure may be very small. However, this requires further examination using population distribution at a finer temporal resolution (e.g., daily and hourly for short-term exposure studies).

4.3. Practical implications of this study

The recent decline in surface $PM_{2.5}$ levels is clearly associated with the environmental policies and control measures enforced by the Chinese government (Cai et al., 2017; Lin et al., 2018). In the 11th Five-Year Plan, a stricter environmental policy was issued to conserve energy and reduce sulfur dioxide (SO_2) emissions from anthropogenic activities (The State Council of China 2006). Thereafter, Air Pollution Prevention and Control policies were enacted in key regions during the 12th Five-Year Plan for 2011–2015, which aimed to reduce energy use, SO_2 and nitrogen oxides (NO_x) emissions (http://www.mee.gov.cn/gkml/hbb/bwj/201212/t20121205_243271.htm). With the increasing occurrence of extremely high $PM_{2.5}$ episodes, the Chinese government recently issued a new version of the NAAQS that for the first time incorporated $PM_{2.5}$ as an air pollutant to be monitored by the national monitoring network (GB3095-2012). Meanwhile, the APPCAP enacted in 2013 introduced a series of control measures with the clear goal of reducing particle pollution (see Section 3.2.2 for the targets in detail). The spatial and temporal analysis in this study could help assess the effectiveness of the policy on the national level, and according to the spatiotemporal analyses in Section 3.2 and 3.3, the overall reduction in $PM_{2.5}$ indicates the clean air targets were almost achieved.

In addition to the national $PM_{2.5}$ reduction, substantial spatiotemporal heterogeneity in the study period is observed, which is

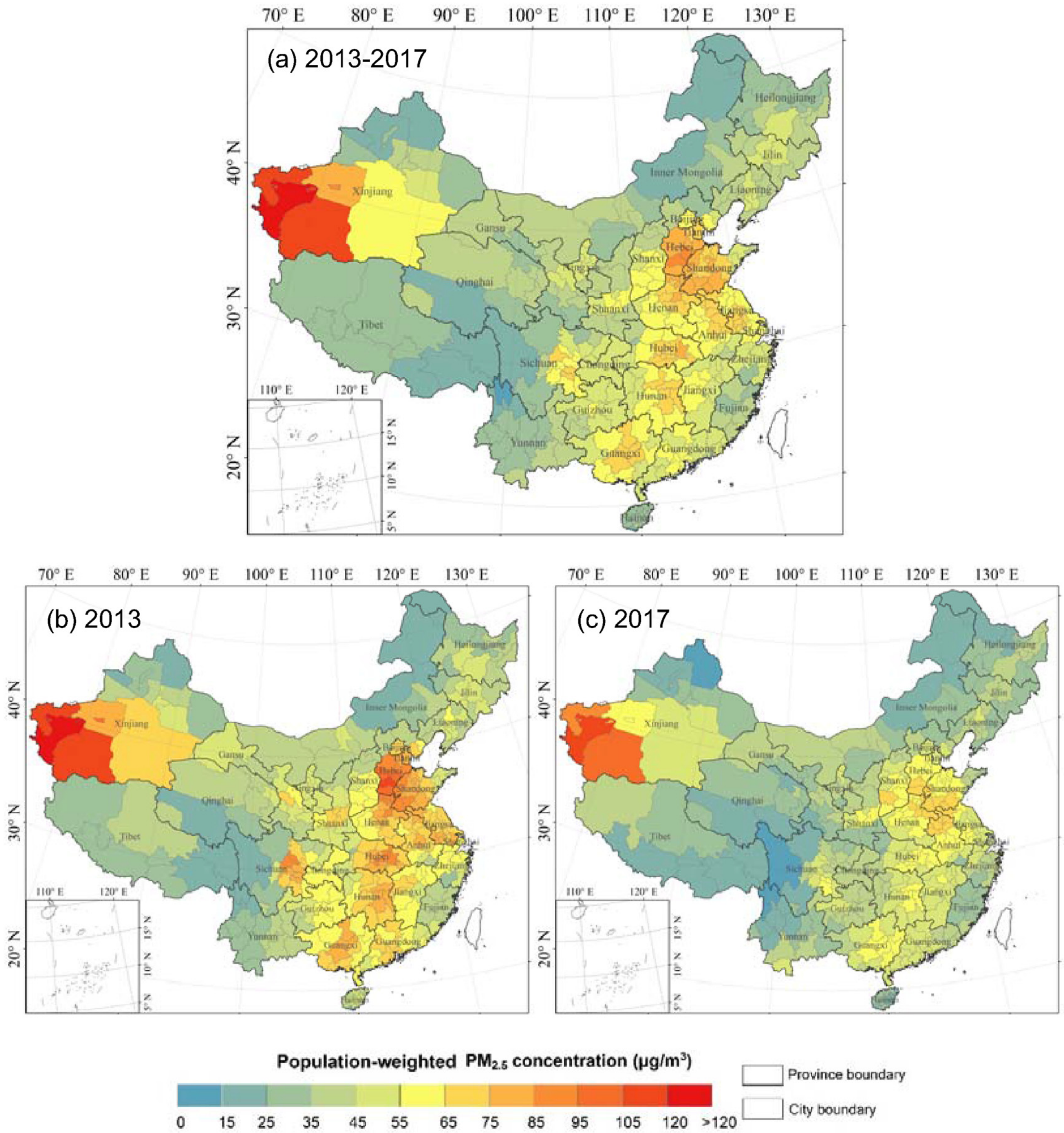

Fig. 5. Spatial distribution of population-weighted mean $PM_{2.5}$ concentrations for each city in China during (a) the 5-year period from 2013 to 2017, (b) 2013, and (c) 2017.

Table 2
2013–2017 p.m.$_{2.5}$ exposure in heavily polluted regions.

Region	Population weighted mean PM2.5 (μg/m^3)			Population at cumulative PM2.5 > 35 μg/m^3 (%)			Population at cumulative PM2.5 > 75 μg/m^3 (%)		
	2013–2017	2013	2017	2013–2017	2013	2017	2013–2017	2013	2017
BTH	70.37	81.25	55.88	96.20	96.83	94.70	42.60	59.03	0.74
YRD	58.08	65.10	49.69	97.78	98.07	94.06	1.66	17.11	1.30
PRD	58.10	68.34	50.82	99.97	99.97	99.63	0.04	12.37	0.02
SCB	54.17	64.13	43.21	96.37	97.83	87.47	1.69	28.29	0.00
Central China	64.11	72.77	52.61	99.16	99.75	94.58	10.19	48.87	0.00

associated with various natural sources and socioeconomic activities (Zhan et al., 2018), individual responses to control policies (Shi et al., 2019) and transboundary air pollution. Because regions have different particle polluted baseline, the environmental strategies to promote low $PM_{2.5}$ concentration development shows apparently a regional difference in performance, which may require additional measures for future control. For instance, by 2017, the majority of China's population, especially those living highly urbanized regions such as the BTH, YRD, PRD, and central China regions, was exposed to risky levels with concentrations exceeding 35 μg/m^3. Further action is thus necessary to mitigate $PM_{2.5}$ pollution, especially in densely populated urban areas.

The comparison results of spatial distribution on $PM_{2.5}$ show that in most cities, there were positive discrepancies between with

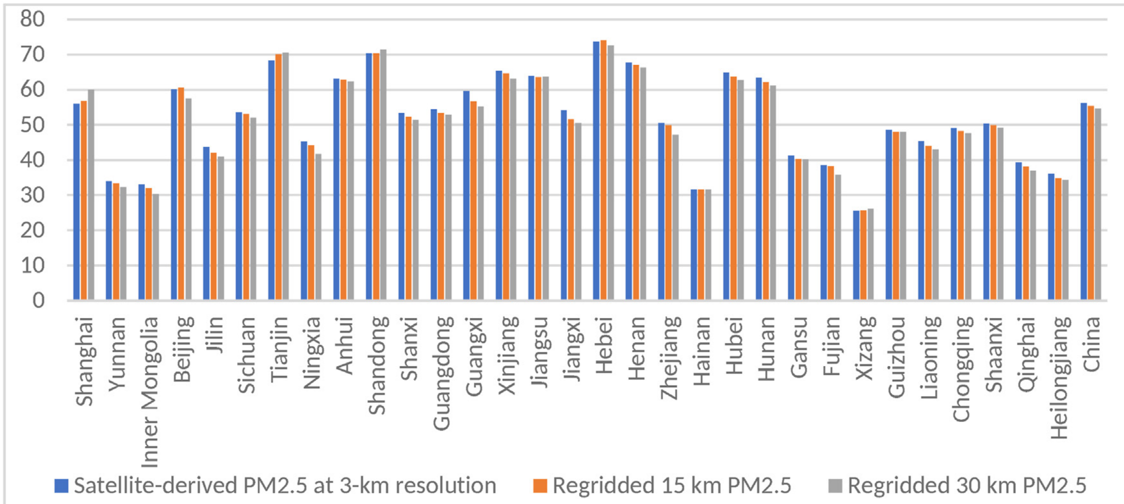

Fig. 6. Population-weighted mean $PM_{2.5}$ concentrations for each province in China at various spatial resolutions from 2013 to 2017.

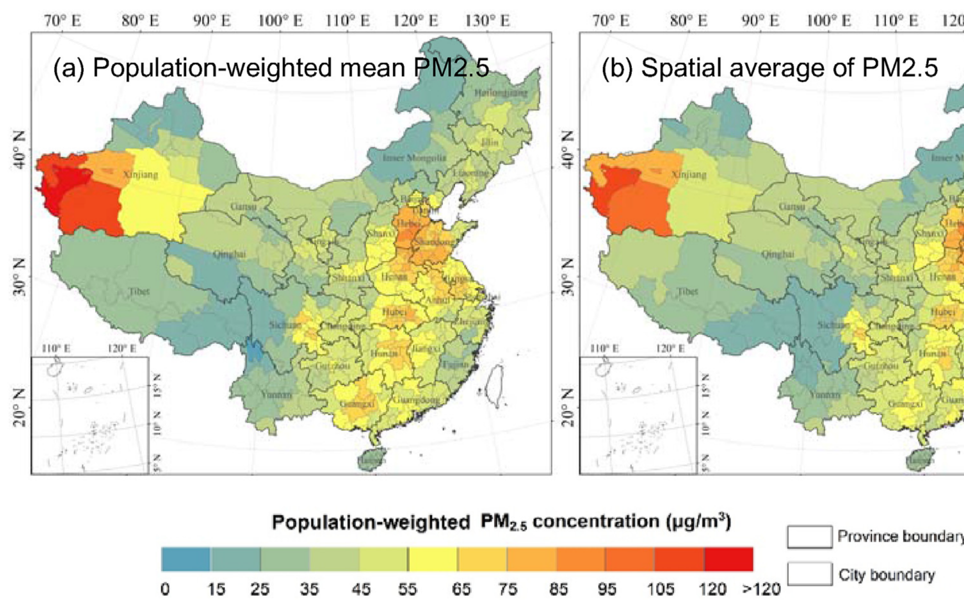

Fig. 7. (a) Spatial distribution of population-weighted average $PM_{2.5}$ concentrations and (b) spatial averages of satellite-derived $PM_{2.5}$ concentrations for various cities for 2013–2017.

and without considering demographic data (Fig. 7). Cities with better air quality would be anticipated if more people were to live in less-polluted areas. However, the higher population-weighted mean $PM_{2.5}$ concentrations relative to those without integrating population data in most Chinese cities suggest that people in China tend to reside in areas with high $PM_{2.5}$ levels, which corresponds with the results of previous studies in which areas with serious $PM_{2.5}$ pollution have been linked to dense populations (He and Huang 2018a; Xie et al., 2015). This exacerbated the intra-city air pollution, highlighting the need for additional city management measures regarding population distribution and environmental quality because the current measures to mitigate air pollution within cities are insufficient to make densely populated areas clean.

The implementation of the current policy has clearly led to a dramatic decrease in local and national $PM_{2.5}$ concentrations. To gain a better understanding of the current status of $PM_{2.5}$ control and future policymaking in China, it is important to take a global perspective and to compare $PM_{2.5}$ levels with those in other countries/regions. The current situation of ambient $PM_{2.5}$ pollution in China is therefore discussed in the context of comparison with Japan, Korea, the United States, and the European Union. There are significant differences in the ambient air quality standard among these five countries/regions. China has promulgated a national standard that aims to meet the Interim Target-1 (IT-1) annual limit of 35 μg/m^3 suggested by the World Health Organization (WHO), whereas the other four have been using stricter $PM_{2.5}$ limits, such as the WHO third-stage IT-3 of 15 μg/m^3 (Table S4). According to Hammer et al. (2020) and Li et al. (2019), these countries/regions have nearly satisfied their national standards, especially Japan, the European Union, and the United States, which generally maintained low $PM_{2.5}$ concentrations from 2013 through 2017, with averages of ~11 μg/m^3, ~11 μg/m^3, and ~6 μg/m^3, respectively (Table S5). However, as discussed in Sections 3.2 and 3.3, most of China was exposed to risky $PM_{2.5}$ pollution above the 35 μg/m^3 standard

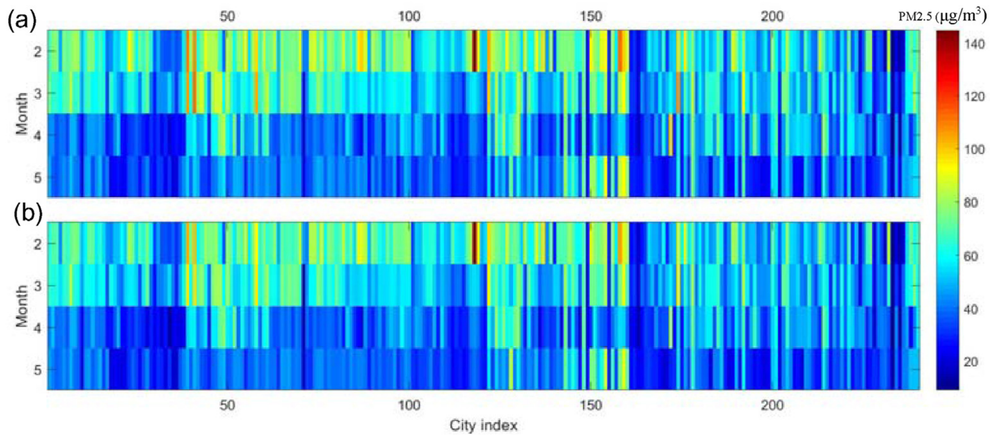

Fig. 8. Monthly population exposure to $PM_{2.5}$ for each city from February to May 2016 using (a) consistent and (b) dynamic population data (city index is displayed in Fig. S8).

throughout the study period despite the enforcement of national and local policies to reduce anthropogenic emissions. As much as the annual concentrations have greatly been reduced in most parts of eastern China, they still far exceed those in the other countries/regions mentioned above (Table S5), due to their differences in energy and industry structures, their stages of urban development, and the status of their natural environment (Li et al., 2019; Shisong et al., 2018). Much effort must still be made for China to limit $PM_{2.5}$ pollution to a lower level, such as the WHO IT-3 of 15 μg/m^3 and the AQG of 10 μg/m^3 (Table S4), and to further reduce the accompanying health risks. Local environmental policies should continue to be implemented and even strengthened. Regional collaborative policies should be considered to control transboundary air pollution. On a grander scale, experiences from other countries/regions in the transformation of industry structure and improvement of the urban and natural environment could be studied and may be applied to further improve future policies on $PM_{2.5}$ control.

In this study, the use of high-resolution $PM_{2.5}$ concentrations allowed us to evaluate $PM_{2.5}$ exposure at the city level with promising implications for better spatial interpretation of the health risks for China. Comparisons based on data using various spatiotemporal resolutions show that the $PM_{2.5}$ exposure assessment would be affected by the spatial resolution and temporal interval. Hence, this study demonstrates the superiority of using fine-scale $PM_{2.5}$ for monitoring air quality and assessing population exposure and further health effects, with direct benefits for not only environmental management but also epidemiological studies.

4.4. Uncertainties and limitations

$PM_{2.5}$ predictions from satellite remote sensing dramatically extend the spatial coverage compared with those from sparsely distributed ground-level monitoring stations, but satellite-derived $PM_{2.5}$ data have missing values induced by the sampling limitations of AOD data associated with the aerosol retrieval algorithm and cloud contamination (Tao et al., 2015). The non-random gaps in the AOD data can result in uncertainties in the prediction model and in the subsequent assessment of population exposure to $PM_{2.5}$ (He and Huang 2018b; Xie et al., 2015). To address this issue, the fused 3-km AOD data were used in this study. With improved sampling frequency compared with the original MODIS 3-km AOD data, the model performance was enhanced to a degree (He and Huang 2018a, b). However, the temporal sampling frequency of the fused 3-km AOD data remained lower than that of ground-level monitors.

To identify the bias pattern caused by the availability of satellite data, the estimated and measured $PM_{2.5}$ concentrations for each monitoring station were compared (Fig. 9). The mean $PM_{2.5}$ estimates for all 1645 days predicted by the GTWR model were on average 5.5 μg/m^3 (15%) higher than the in situ mean concentrations for all measured days throughout the 2013–2017 timespan. For the discrepancies between the 5-year mean satellite-based and ground-observed concentrations, more than 50% of monitors fell within the bias level of ±10 μg/m^3 (Fig. 9 (a)), whereas more than 60% of sites had a mean difference ratio of less than ±20% (Fig. 9 (b)). Therefore, the satellite remote sensing $PM_{2.5}$ estimates used in this study generally showed good agreement with the surface observations and show promise for characterization of the spatiotemporal variations in $PM_{2.5}$ pollution and exposure at the national scale. However, Fig. 9 (b) and (c) also show distinct regional differences in bias among provinces, with particularly obvious discrepancies in Xinjiang (negative differences) and Guangdong (positive differences). The bias appears to be concentrated in areas where the particle mass varied significantly over time and the satellite AOD data coverage was lower than in the neighboring areas (see Fig. S2 for the sampling frequency of fused 3-km AOD data). This implies that the evaluation of long-term $PM_{2.5}$ exposure in this study was probably slightly higher in the southern cities and lower in the northwestern areas, and also highlights the importance of further improvement in the availability of fine-scale AOD data.

Other possible errors in the ground $PM_{2.5}$ predictions include those from the multiresolution variable data and the fusion method. The integration of multisource predictors with varying spatial scales and temporal intervals may have introduced uncertainties into the relationship between $PM_{2.5}$ and AOD. For instance, the percentage of artificial surface from land use data collected in 2010 was derived to represent the entire study period of 2013–2017. As these data did not take account of the changes in land use over the 5 years, it is likely that the contribution of such changes was reduced in the spatiotemporal modeling. However, it is difficult to obtain land-use data collocated to the study years due to the limited data availability. If possible, land-use data with a higher temporal resolution would be used in future studies, and the difference between multiple types of data would be quantitatively analyzed. Furthermore, the fusion method improved the data availability of the high-resolution AOD but brought additional uncertainties into the 3-km aerosol data. To quantify the difference between the fused and MODIS original 3-km AOD, the two datasets against the ground-level aerosol observations for each monitoring

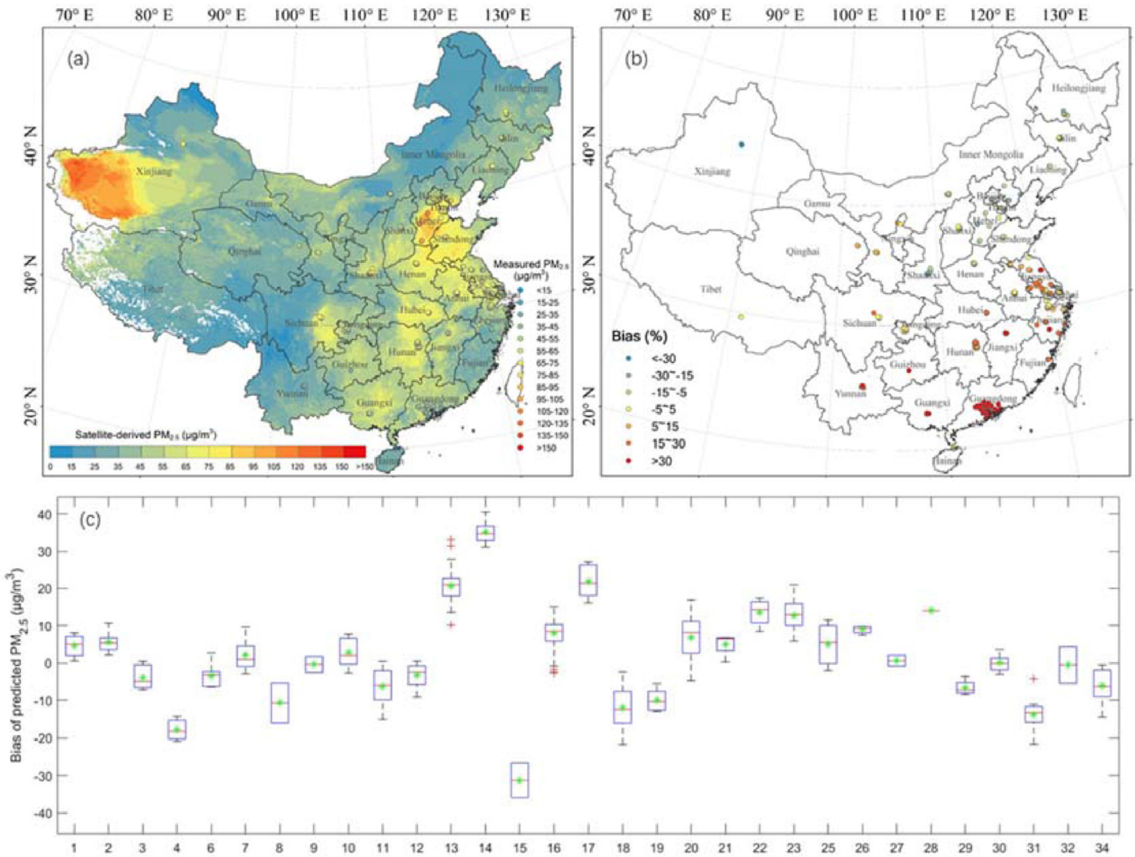

Fig. 9. (a) Satellite-derived and monitor-based mean $PM_{2.5}$ concentrations from 2013 to 2017, (b) mean percentage, and (c) boxplot of bias between estimated and measured $PM_{2.5}$ concentrations at each site. The boxplot uses the first and third quartiles grouped by province, and the green asterisk in the box represents the mean bias for each province. Note that only sites that provided more than 1500 valid values (corresponding to 300 values per year) were used for this evaluation (N = 290). The $PM_{2.5}$ concentration was estimated based on those days when AOD values were available and the measured $PM_{2.5}$ concentration was based on all measured days. (For interpretation of the references to colour in this figure legend, the reader is referred to the Web version of this article.)

site were compared; the results are summarized in Table S3. Although the accuracy of the fused 3-km AOD was generally competitive with the MODIS operational AOD in Fig. S2, the fused data led to slightly different levels of precision in different areas: accuracy improved in certain areas (e.g., Beijing site for Aqua and Terra) and worsened in others (e.g., Hong Kong site for Aqua). Therefore, future studies aiming to improve AOD should have not only better sampling frequency but also greater accuracy.

5. Conclusions and future prospects

This study explored the spatiotemporal patterns and dynamics of $PM_{2.5}$ pollution in China from 2013 to 2017 using a fine spatial-scale $PM_{2.5}$ sequence estimated via spatiotemporal modeling. The overall trends and spatial variations in the population-weighted mean $PM_{2.5}$ concentration were also used as a proxy to investigate spatiotemporal changes in the health effects of $PM_{2.5}$ exposure on the population. Spatially, the overall concentration of ambient $PM_{2.5}$ in China decreased from 2013 to 2017 with significant spatial variability, and temporally, it changed remarkably from 2013 to 2014 to 2015–2017. The overall proportion of the population exposed to extreme particulate levels (>75 $\mu g/m^3$) declined sharply from 2013 to 2017, but most of China's population was still exposed to sustained risky levels (>35 $\mu g/m^3$) over the 5 study years, especially in densely populated areas such as the BTH region. The decrease was related to a series of control policies under the APPCAP introduced by the Chinese government to ensure cleaner air. The BTH and PRD regions reached the goals set by the APPCAP, and YRD was close to the target. However, our findings suggest that ambient $PM_{2.5}$ pollution still poses a serious health risk to the Chinese population, and that additional measures are still urgently needed to further improve China's air quality in the coming years.

This study also explored how estimates of $PM_{2.5}$ exposure can be affected by varying the spatial scale of the $PM_{2.5}$ data and varying the temporal interval of the population distribution. The comparison results show that coarse-resolution $PM_{2.5}$ estimates tend to underestimate exposure and obscure considerable spatial details about health risk, which underlines the benefit of the use of high-resolution $PM_{2.5}$ data for environmental management and epidemiological studies. In contrast, the temporal dynamics of population distribution show little influence on the assessment of $PM_{2.5}$ exposure on a monthly scale. As a pioneering high-resolution spatiotemporal $PM_{2.5}$ exposure analysis with a focus on the 2013–2017 period, when the APPCAP was implemented across China, the findings of this study provide effective information to guide future measures to mitigate $PM_{2.5}$ pollution and thus facilitate a reduction in the morbidity and death induced by $PM_{2.5}$ in China.

However, future studies of $PM_{2.5}$ exposure assessment with the use of satellite-derived data are still warranted. The use of better aerosol data, such as those derived from the 1-km MAIAC AOD dataset or improved by new fusion methods, should be further promoted to obtain more representative $PM_{2.5}$ mass concentration data for exposure assessment. In addition, more elaborate demographic data will be indispensable for better quantitative analysis of $PM_{2.5}$ exposure because further examination is required with finer timescale population data to assess the short-term effects of exposure.

Author contributions

HE Q. and HUANG B. designed the whole experiment. HE Q. developed the experiment code and performed it. SONG Y. provided geospatial big data. The paper was initially written by HE Q. and significantly revised by ZHANG M., and ZHANG M. and HUANG B. provided a lot of constructive comments on the experiment.

Declaration of competing interest

The authors declare that they have no known competing financial interests or personal relationships that could have appeared to influence the work reported in this paper.

Acknowledgments

This study was supported by the National Natural Science Foundation of China (Grant NO. 41901324, 52079101, 42001385) and the Fundamental Research Funds for the Central Universities (WUT: 193108007). We thank Qingyue Open Environmental Data Center for supporting part of the observed $PM_{2.5}$ data.

Appendix A. Supplementary data

Supplementary data to this article can be found online at https://doi.org/10.1016/j.jclepro.2020.124965.

References

Barnett, A.G., Williams, G.M., Schwartz, J., Best, T.L., Neller, A.H., Petroeschevsky, A.L., Simpson, R.W., 2006. The effects of air pollution on hospitalizations for cardiovascular disease in elderly people in Australian and New Zealand cities. Environ. Health Perspect. 114, 1018.
Bai, K., Ma, M., Chang, N.B., Gao, W., 2019. Spatiotemporal trend analysis for fine particulate matter concentrations in China using high-resolution satellite-derived and ground-measured PM2. 5 data. J. Environ. Manag. 233, 530–542.
Cai, S., Wang, Y., Zhao, B., Wang, S., Chang, X., Hao, J., 2017. The impact of the "air pollution prevention and control action plan" on PM2.5 concentrations in jing-jin-ji region during 2012–2020. Sci. Total Environ. 580, 197–209.
Chen, B., Song, Y., Jiang, T., Chen, Z., Huang, B., Xu, B., 2018. Real-time estimation of population exposure to PM2.5 using mobile- and station-based big data. Int. J. Environ. Res. Publ. Health *15*.
Chen, Y., Ebenstein, A., Greenstone, M., Li, H., 2013. Evidence on the impact of sustained exposure to air pollution on life expectancy from China's Huai River policy. Proc. Natl. Acad. Sci. Unit. States Am. 110, 12936.
Chudnovsky, A.A., Koutrakis, P., Kloog, I., Melly, S., Nordio, F., Lyapustin, A., Wang, Y., Schwartz, J., 2014. Fine particulate matter predictions using high resolution Aerosol Optical Depth (AOD) retrievals. Atmos. Environ. 89, 189–198.
van Donkelaar, A., Martin, R.V., Brauer, M., Hsu, N.C., Kahn, R.A., Levy, R.C., Lyapustin, A., Sayer, A.M., Winker, D.M., 2016. Global estimates of fine particulate matter using a combined geophysical-statistical method with information from satellites, models, and monitors. Environ. Sci. Technol. 50, 3762–3772.
Fang, X., Zou, B., Liu, X., Sternberg, T., Zhai, L., 2016. Satellite-based ground PM 2.5 estimation using timely structure adaptive modeling. Rem. Sens. Environ. 186, 152–163.
Fu, J., Jiang, D., Huang, Y., 2014. KM grid population dataset of China (PopulationGrid_China). *Global Change Research Data Publishing & Repository*.
Gu, Y., Wong, T.W., Law, C.K., Dong, G.H., Ho, K.F., Yang, Y., Yim, S.H.L., 2018. Impacts of sectoral emissions in China and the implications: air quality, public health, crop production, and economic costs. Environ. Res. Lett. 13, 084008.
Gui, K., Che, H., Wang, Y., Wang, H., Zhang, L., Zhao, H., et al., 2019. Satellite-derived PM2. 5 concentration trends over Eastern China from 1998 to 2016: relationships to emissions and meteorological parameters. Environ. Pollut. 247, 1125–1133.
Guo, H., Cheng, T., Gu, X., Wang, Y., Chen, H., Bao, F., Shi, S., Xu, B., Wang, W., Zuo, X., 2017a. Assessment of PM2. 5 concentrations and exposure throughout China using ground observations. Sci. Total Environ. 601, 1024–1030.
Guo, Y., Tang, Q., Gong, D.-Y., Zhang, Z., 2017b. Estimating ground-level PM2. 5 concentrations in Beijing using a satellite-based geographically and temporally weighted regression model. Rem. Sens. Environ. 198, 140–149.
Hammer, M.S., van Donkelaar, A., Li, C., Lyapustin, A., Sayer, A.M., Hsu, N.C., et al., 2020. Global estimates and long-term trends of fine particulate matter concentrations (1998-2018). Environ. Sci. Technol. 54 (13), 7879–7890.
He, Q., Gu, Y., Zhang, M., 2019. Spatiotemporal patterns of aerosol optical depth throughout China from 2003 to 2016. Sci. Total Environ. 653, 23–35.
He, Q., Huang, B., 2018a. Satellite-based high-resolution PM2.5 estimation over the Beijing-Tianjin-Hebei region of China using an improved geographically and temporally weighted regression model. Environ. Pollut. 236, 1027–1037.
He, Q., Huang, B., 2018b. Satellite-based mapping of daily high-resolution ground PM 2.5 in China via space-time regression modeling. Rem. Sens. Environ. 206, 72–83.
Hu, X., Waller, L.A., Lyapustin, A., Wang, Y., Al-Hamdan, M.Z., Crosson, W.L., Liu, Y., 2014. Estimating ground-level PM2. 5 concentrations in the Southeastern United States using MAIAC AOD retrievals and a two-stage model. Rem. Sens. Environ. 140, 220–232.
Huang, B., Wu, B., Barry, M., 2010. Geographically and temporally weighted regression for modeling spatio-temporal variation in house prices. Int. J. Geogr. Inf. Sci. 24, 383–401.
Huang, J., Pan, X., Guo, X., Li, G., 2018. Health impact of China's Air Pollution Prevention and Control Action Plan: an analysis of national air quality monitoring and mortality data. The Lancet Planetary Health 2 (7), e313–e323.
Lee, H.J., Chatfield, R.B., Strawa, A.W., 2016. Enhancing the applicability of satellite remote sensing for PM2. 5 estimation using MODIS deep blue AOD and land use regression in California, United States. Environ. Sci. Technol. 50 (12), 6546–6555.
Levy, R., Mattoo, S., Munchak, L., Remer, L., Sayer, A., Hsu, N., 2013. The Collection 6 MODIS aerosol products over land and ocean. Atmos. Meas. Tech. Discuss 6, 159–259.
Li, J., Han, X., Jin, M., Zhang, X., Wang, S., 2019. Globally analysing spatiotemporal trends of anthropogenic PM2. 5 concentration and population's PM2. 5 exposure from 1998 to 2016. Environ. Int. 128, 46–62.
Li, T., Shen, H., Zeng, C., Yuan, Q., Zhang, L., 2017. Point-surface fusion of station measurements and satellite observations for mapping PM 2.5 distribution in China: methods and assessment. Atmos. Environ. 152, 477–489.
Liang, F., Xiao, Q., Wang, Y., Lyapustin, A., Li, G., Gu, D., et al., 2018. MAIAC-based long-term spatiotemporal trends of PM2. 5 in Beijing, China. Sci. Total Environ. 616, 1589–1598.
Lin, C., Liu, G., Lau, A., Li, Y., Li, C., Fung, J., Lao, X., 2018. High-resolution satellite remote sensing of provincial PM2. 5 trends in China from 2001 to 2015. Atmos. Environ. 180, 110–116.
Ma, Z., Liu, Y., Zhao, Q., Liu, M., Zhou, Y., Bi, J., 2016. Satellite-derived high resolution PM 2.5 concentrations in Yangtze River Delta Region of China using improved linear mixed effects model. Atmos. Environ. 133, 156–164.
Peng, J., Chen, S., Lü, H., Liu, Y., Wu, J., 2016. Spatiotemporal patterns of remotely sensed PM 2.5 concentration in China from 1999 to 2011. Rem. Sens. Environ. 174, 109–121.
Remer, L., Mattoo, S., Levy, R., Munchak, L., 2013. MODIS 3 km aerosol product: algorithm and global perspective. Atmospheric Measurement Techniques 6, 1829–1844.
Schwartz, J., 1996. Air pollution and hospital admissions for respiratory disease. Epidemiology 20–28.
Shi, H., Wang, S., Guo, S., 2019. Predicting the impacts of psychological factors and policy factors on individual's PM2. 5 reduction behavior: an empirical study in China. J. Clean. Prod. 241, 118416.
Shisong, C., Wenji, Z., Hongliang, G., Deyong, H., You, M., Wenhui, Z., Shanshan, L., 2018. Comparison of remotely sensed PM2. 5 concentrations between developed and developing countries: results from the US, Europe, China, and India. J. Clean. Prod. 182, 672–681.
Tao, M., Chen, L., Wang, Z., Tao, J., Che, H., Wang, X., Wang, Y., 2015. Comparison and evaluation of the MODIS Collection 6 aerosol data in China. J. Geophys. Res.: Atmosphere 120, 6992–7005.
The State Council of China, 2013. Air Pollution Prevention and Control Action Plan [In Chinese]. http://www.gov.cn/zwgk/2013-09/12/content_2486773.htm.
Tiao, G., Reinsel, G., Xu, D., Pedrick, J., Zhu, X., Miller, A., DeLuisi, J., Mateer, C., Wuebbles, D., 1990. Effects of autocorrelation and temporal sampling schemes on estimates of trend and spatial correlation. J. Geophys. Res.: Atmosphere 95, 20507–20517, 1984–2012.
Wang, B., Shi, W., Miao, Z., 2015. Confidence analysis of standard deviational ellipse and its extension into higher dimensional Euclidean space. PloS One 10, e0118537.
Wang, J., Zhang, L., Niu, X., Liu, Z., 2020. Effects of PM2.5 on health and economic loss: evidence from Beijing-Tianjin-Hebei region of China. J. Clean. Prod. 257, 120605.
Weatherhead, E.C., Reinsel, G.C., Tiao, G.C., Meng, X.L., Choi, D., Cheang, W.K., Keller, T., DeLuisi, J., Wuebbles, D.J., Kerr, J.B., 1998. Factors affecting the detection of trends: statistical considerations and applications to environmental data. J. Geophys. Res.: Atmosphere 103, 17149–17161, 1984–2012.
Wei, J., Huang, W., Li, Z., Xue, W., Peng, Y., Sun, L., Cribb, M., 2019a. Estimating 1-km-resolution PM2. 5 concentrations across China using the space-time random forest approach. Rem. Sens. Environ. 231, 111221.
Wei, J., Li, Z., Cribb, M., Huang, W., Xue, W., Sun, L., Guo, J., Peng, Y., Li, J., Lyapustin, A., Liu, L., Wu, H., Song, Y., 2020. Improved 1 km resolution PM2.5 estimates across China using enhanced space–time extremely randomized trees. Atmos. Chem. Phys. 20, 3273–3289.

Wu, J., Yao, F., Li, W., Si, M., 2016. VIIRS-based remote sensing estimation of ground-level PM 2.5 concentrations in Beijing–Tianjin–Hebei: a spatiotemporal statistical model. Rem. Sens. Environ. 184, 316–328.
Xiao, Q., Wang, Y., Chang, H.H., Meng, X., Geng, G., Lyapustin, A., Liu, Y., 2017. Full-coverage high-resolution daily PM2.5 estimation using MAIAC AOD in the Yangtze River Delta of China. Rem. Sens. Environ. 199, 437–446.
Xie, Y., Wang, Y., Zhang, K., Dong, W., Lv, B., Bai, Y., 2015. Daily estimation of ground-level PM2. 5 concentrations over Beijing using 3 km resolution MODIS AOD. Environ. Sci. Technol. 49, 12280–12288.
Xue, T., Liu, J., Zhang, Q., Geng, G., Zheng, Y., Tong, D., et al., 2019a. Rapid improvement of PM 2.5 pollution and associated health benefits in China during 2013–2017. Sci. China Earth Sci. 62 (12), 1847–1856.
Xue, T., Zheng, Y., Tong, D., Zheng, B., Li, X., Zhu, T., Zhang, Q., 2019b. Spatiotemporal continuous estimates of PM2.5 concentrations in China, 2000-2016: a machine learning method with inputs from satellites, chemical transport model, and ground observations. Environ. Int. 123, 345–357.
Xue, W., Zhang, J., Zhong, C., Ji, D., Huang, W., 2020. Satellite-derived spatiotemporal PM2. 5 concentrations and variations from 2006 to 2017 in China. Sci. Total Environ. 712, 134577.
Yang, L., Xu, H., Jin, Z., 2019. Estimating ground-level PM2. 5 over a coastal region of China using satellite AOD and a combined model. J. Clean. Prod. 227, 472–482.
You, W., Zang, Z., Zhang, L., Li, Y., Wang, W., 2016. Estimating national-scale ground-level PM25 concentration in China using geographically weighted regression based on MODIS and MISR AOD. Environ. Sci. Pollut. Control Ser. 23, 8327–8338.
Zhan, D., Kwan, M.P., Zhang, W., Yu, X., Meng, B., Liu, Q., 2018. The driving factors of air quality index in China. J. Clean. Prod. 197, 1342–1351.
Zhang, Q., Zheng, Y., Tong, D., Shao, M., Wang, S., Zhang, Y., et al., 2019. Drivers of improved PM2. 5 air quality in China from 2013 to 2017. Proc. Natl. Acad. Sci. Unit. States Am. 116 (49), 24463–24469.